The Astrophysical Journal, 710:698–705, 2010 February 10 doi:10.1088/0004-637X/710/1/698

EVIDENCE FOR INFRARED-FAINT RADIO SOURCES AS $z > 1$ RADIO-LOUD ACTIVE GALACTIC NUCLEI

Minh T. Huynh[1], Ray P. Norris[2], Brian Siana[3], and Enno Middelberg[4]
[1] Infrared Processing and Analysis Center, MS 220-6, California Institute of Technology, Pasadena, CA 91125, USA; mhuynh@ipac.caltech.edu
[2] Australia Telescope National Facility, CSIRO, Epping, NSW 1710, Australia
[3] California Institute of Technology, MS 105-24, Pasadena, CA 91125, USA
[4] Astronomisches Institut, Ruhr-Universitat Bochum, Universitatsstr. 150, 44801 Bochum, Germany
Received 2009 May 29; accepted 2009 December 2; published 2010 January 21

ABSTRACT

Infrared-Faint Radio Sources (IFRSs) are a class of radio objects found in the Australia Telescope Large Area Survey which have no observable mid-infrared counterpart in the *Spitzer* Wide-area Infrared Extragalactic (SWIRE) survey. The extended Chandra Deep Field South now has even deeper *Spitzer* imaging (3.6–70 μm) from a number of Legacy surveys. We report the detections of two IFRS sources in IRAC images. The non-detection of two other IFRSs allows us to constrain the source type. Detailed modeling of the spectral energy distribution of these objects shows that they are consistent with high-redshift ($z \gtrsim 1$) active galactic nuclei.

Key words: galaxies: evolution – galaxies: formation – galaxies: starburst

Online-only material: color figure

1. INTRODUCTION

Infrared-Faint Radio Sources (IFRSs) were recently discovered in the Australia Telescope Large Area Survey (ATLAS) by Norris et al. (2006). These are radio sources brighter than a few hundred μJy at 1.4 GHz which have no observable infrared counterpart in the *Spitzer* Wide-area Infrared Extragalactic Survey (SWIRE; Lonsdale et al. 2004). They may be related to the optically invisible radio sources found by Higdon et al. (2005, 2008), which are compact radio sources with no optical counterpart to $R \sim 25.7$.

Norris et al. (2006) and Middelberg et al. (2008b) have identified 53 such sources out of 2002 radio sources in ATLAS. Most have flux densities of a few hundred μJy at 1.4 GHz, but some are as bright as 20 mJy. The IFRS sources were unexpected as SWIRE was thought to be deep enough to detect all radio sources in the local universe, regardless of whether star formation or active galactic nuclei (AGNs) powered the radio emission. Possible explanations are that these sources are (1) extremely high-redshift ($z > 3$) radio-loud AGNs, (2) very obscured radio galaxies at more moderate redshifts ($1 < z < 2$), (3) lobes of nearby but unidentified radio galaxies, or (4) an unknown type of object.

The nature of IFRSs has been hard to determine because they have only been detected in the radio. Spectroscopy is difficult because the hosts are optically faint and the radio positions can also have uncertainties on the order of a few arcseconds. Norris et al. (2006) stacked the positions of 22 IFRSs in the *Spitzer* 3.6 μm IRAC images and found no detection in the averaged image, showing that they are well below the SWIRE detection threshold.

Recently, Middelberg et al. (2008a) and Norris et al. (2007) targeted six IFRSs with the Australian Long Baseline Array (LBA) and successfully detected two of the sources. The Norris et al. (2007) LBA detection constrained the source size to less than 0.03 arcsec, suggesting a compact radio core powered by an AGN. Middelberg et al. (2008a) found the size and radio luminosity of their LBA-detected source to be consistent with a high-redshift ($z > 1$) Compact Steep Spectrum Source. The VLBI detections rule out the possibility that these particular IFRSs are simply the radio lobes of unidentified radio galaxies. Garn & Alexander (2008) stacked IFRS sources in the *Spitzer* First Look Survey at infrared wavelengths as well as at 610 MHz. They find that the IFRS sources can be modeled as compact Fanaroff–Riley type II (FR II) radio galaxies at high redshift ($z \sim 4$). Thus, the evidence suggests that IFRSs are predominately high-redshift radio-loud AGNs.

Ultra-deep *Spitzer* imaging is now available over the 30×30 arcmin^2 region of the Chandra Deep Field South SWIRE field. Four IFRSs lie in this region and in this paper we report on the constraints on the nature of IFRSs derived from the new *Spitzer* data. We assume a Hubble constant of 71 km s^{-1} Mpc^{-1}, and matter and cosmological constant density parameters of $\Omega_M = 0.27$ and $\Omega_\Lambda = 0.73$ in this paper.

2. OBSERVATIONS, DATA, AND SAMPLE SELECTION

The extended Chandra Deep Field South (eCDFS) is centered at $3^h32^m28^s$, $-27°48'30''$. It overlaps the Great Observatories Origins Deep Survey (GOODS) South field, which is one of the best studied regions of the sky. ATLAS (Norris et al. 2006) consists of deep radio observations of a 3.7 deg^2 field surrounding the eCDFS which is coincident with SWIRE (Lonsdale et al. 2004). The ATLAS 1.4 GHz observations reach 20–60 μJy rms, with the deepest region covering the 30×30 arcmin^2 eCDFS. ATCA 2.4 GHz observations of the SWIRE region were obtained by the ATLAS team over the last two years and the current image reaches ~0.1 mJy rms (E. Middelberg et al. 2010, in preparation).

The SWIRE survey reaches 5σ depths of 3.5, 7.0, 41, and 49 μJy, respectively, in the four IRAC bands (Lonsdale et al. 2004). In the MIPS bands at 24 and 70 μm, the SWIRE 5σ depths are 189 μJy and 16 mJy. To these depths, 22 radio sources in the full SWIRE Chandra Deep Field South region were undetected, and classed as IFRS (Norris et al. 2006). This paper focuses on four IFRS sources which lie in the 30×30 arcmin^2 region of the eCDFS.

The eCDFS subregion of SWIRE has been the target of two separate *Spitzer* Legacy proposals since SWIRE, and hence there are now deeper infrared data. The "*Spitzer* IRAC MUSYC Public Legacy in E-CDFS" (SIMPLE) Legacy project

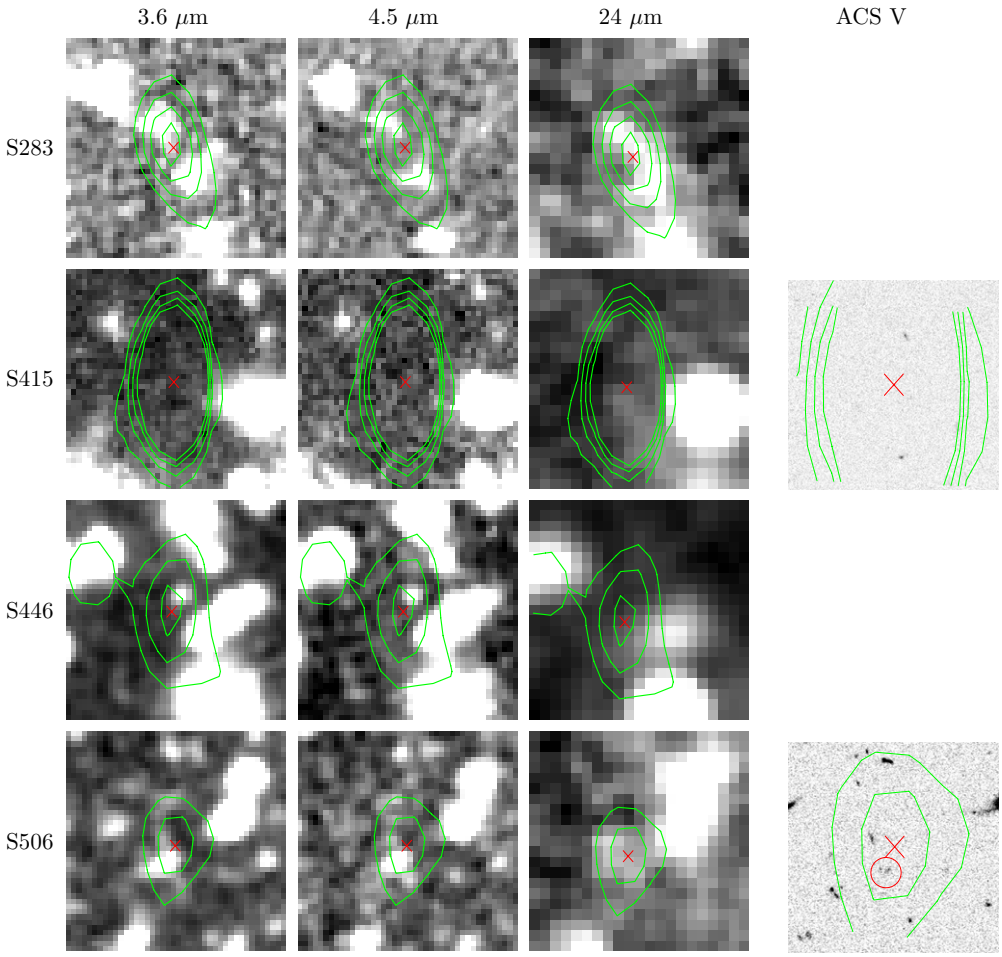

Figure 1. Gray scale *Spitzer* and ACS images of S283, S415, S446, and S506. From left to right, images are IRAC 3.6, 4.5 μm, MIPS 24 μm, and ACS *V* band. The ACS gray scale is inverted for clarity. The green contours are the radio 1.4 GHz image with levels set at 50, 100, 150, and 200 μJy. The red cross marks the radio position. The *Spitzer* images are 25 × 25 arcsec and the ACS image is 12.5 × 12.5 arcsec. The IRAC counterpart to S446 can be seen 2.2 arcsec north of the radio position. The red circle in the S506 ACS image marks the very faint optical counterpart, which is consistent with the proposed IRAC counterpart 2 arcsec south of the radio position.

(M. Damen et al. 2010, in preparation) provides ultra-deep imaging of eCDFS in all four IRAC bands, and the "Far-Infrared Deep Extragalactic Legacy" (FIDEL; PI: Dickinson) Legacy project adds ultra-deep 24 and 70 μm observations. The 5σ depths of SIMPLE are about 0.8, 1.2, 6.3, and 6.6 μJy in IRAC channels 1–4, respectively. FIDEL achieves 5σ depths of 50 μJy and 3 mJy at 24 and 70 μm, respectively, in the areas with most coverage. We searched for counterparts to the four IFRS sources in the new *Spitzer* data. A matching radius of up to 3 arcsec was used for the IRAC and MIPS 24 μm data, and 8 arcsec for MIPS 70 μm. All four positions were examined by eye in all *Spitzer* bands for any obvious failures (see Figure 1). We find two of the sources (S446 and S506) were detected in the SIMPLE ultra-deep IRAC imaging (see Figure 1) and we have improved IR constraints for the rest. Table 1 summarizes the data for the four IFRSs.

We have also searched for counterparts in existing deep optical and near-infrared (NIR) data of the eCDFS from GOODS (Giavalisco et al. 2004), GEMS (Rix et al. 2004), and MUSYC (Gawiser et al. 2006), and find an optical/NIR detection of only one IFRS source (S506). The GOODS ACS imaging reaches approximately $B_{\rm AB} = 28.1$, $V_{\rm AB} = 28.9$, $I_{\rm AB} = 28.3$, and $z_{\rm AB} = 27.4$. GEMS comprises two band ACS imaging and reaches depths of $V_{\rm AB} = 28.25$ and $z_{\rm AB} = 27.1$. The MUSYC survey has a 5σ sensitivity of about $J_{\rm AB} \sim 22.5$ and $K_{\rm AB} \sim 22.0$ (Taylor et al. 2009). Two IFRSs, S415 and S506, lie within the deep optical/NIR imaging area and only one, S506, is detected as a very faint source. The lack of a detection in these optical and NIR images for S415 strongly implies that it is at high redshift and/or is very obscured.

A 2 Ms X-ray exposure of GOODS-South was obtained with the *Chandra X-ray Observatory* (Giacconi et al. 2002; Luo et al. 2008). The on-axis full band sensitivity reaches 7.1×10^{-17} erg s^{-1} cm^{-2} at the average aim point and the minimum full band sensitivity is about 3.3×10^{-16} erg s^{-1} cm^{-2} over the GOODS-S region. Only one of the IFRS sources (S415) lies within the X-ray coverage and there is no detection.

The photometry of the IFRSs was fitted with the following templates: (1) a prototypical starburst ULIRG (Arp 220; Silva et al. 1998), (2) a hot dusty AGN-dominated ULIRG (Mrk 231, photometry from NED[5]), (3) a star-forming M82-like galaxy (Chary & Elbaz 2001), (4) a radio-loud galaxy with an extreme radio–optical ratio (3C273, photometry from NED), and (5) an old stellar population from Maraston (2005). The old stellar

[5] http://nedwww.ipac.caltech.edu/. The NASA/IPAC Extragalactic Database (NED) is operated by the Jet Propulsion Laboratory, California Institute of Technology, under contract with the National Aeronautics and Space Administration.

Table 1
Summary of the Observed Properties of the Four IFRSs in the Extended Chandra Deep Field South

Property	S283	S415	S446	S506
R.A. (J2000)	3:30:48.686	3:32:13.077	3:32:31.540	3:33:11.486
Decl. (J2000)	−27:44:45.32	−27:43:51.07	−28:04:33.53	−28:03:19.09
Radio 1.4 GHz	0.287 mJy	1.21 mJy	0.338 mJy	0.170 mJy
Radio 2.4 GHz	<0.40 mJy	0.67 mJy	<0.45 mJy	<0.45 mJy
$\alpha_{1.4\,\mathrm{GHz}}^{2.5\,\mathrm{GHz}}$ ($S \propto \nu^{\alpha}$)	<0.6	-1.1 ± 0.13	<0.5	<1.8
ACS B mag	...	>28.1	...	...
ACS V mag	...	>28.9	...	26.27
ACS I mag	...	>28.3	...	...
ACS z mag	...	>27.4	...	25.62
SWIRE g′ mag	...	...	>25.3	...
SWIRE r′ mag	...	...	>24.8	...
SWIRE i′ mag	...	...	>23.7	...
J mag	...	>25.5	...	>22.5
H mag	...	>25.8	...	...
K mag	...	>25.5	...	>22.0
IRAC 3.6 μm	<3.5 μJy	<0.8 μJy	6.6 ± 0.3 μJy	5.5 ± 0.3 μJy
IRAC 4.5 μm	<7.0 μJy	<1.2 μJy	5.7 ± 0.5 μJy	5.5 ± 0.4 μJy
IRAC 5.8 μm	<41 μJy	<6.3 μJy	<6.3 μJy	<6.3 μJy
IRAC 8.0 μm	<49 μJy	<6.6 μJy	<6.6 μJy	<6.6 μJy
MIPS 24 μm	<100 μJy	<50 μJy	<80 μJy	<80 μJy
MIPS 70 μm	<16 mJy	<3 mJy	<5 mJy	<5 mJy

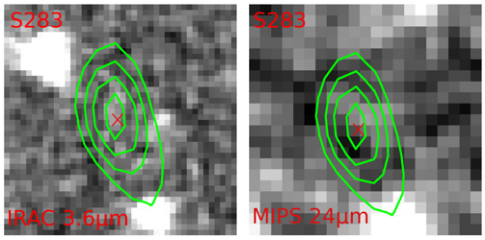

Figure 2. Residual image for S283 with the two point sources near the radio center removed, for IRAC 3.6 μm (left) and MIPS 24 μm (right). As for Figure 1, the green contours are the radio 1.4 GHz image with levels set at 50, 100, 150, and 200 μJy, and the red cross marks the radio position. There is very little IRAC or MIPS flux at the radio position.

templates were fitted only to the two IFRS sources with IRAC detections (S446 and S506). The Maraston (2005) templates explored have a metallicity of 0.67, assume a Salpeter initial mass function, and have ages of 0.3, 1, and 5 Gyr. The results of the spectral energy distribution (SED) analysis are described in the following section.

3. DISCUSSION

3.1. S283

This 0.287 mJy radio source lies just outside of the SIMPLE ultra-deep IRAC imaging and FIDEL 70 μm imaging. There are no SWIRE optical data either, but the shallower SWIRE IRAC 3.6 and 4.5 μm imaging shows the radio source is positioned between two IRAC sources (Figure 1), which are 3.5 and 3.7 arcsec offset, respectively. The offsets are large (>5 times the uncertainty of the radio position), so we do not consider either IRAC source to be a plausible counterpart. The FIDEL 24 μm imaging shows some possible flux at the source position, but it is likely that this faint flux is confusion from the two nearby IRAC sources. To verify that there is no detection of the radio source in the IRAC and MIPS 24 μm bands the two point sources were subtracted from the images and the residual image is shown in Figure 2. The residual flux at the radio position is 2.4 ± 1.8 μJy at 3.6 μm and 13 ± 7 μJy at 24 μm. This is consistent with the conservative upper limits we have assumed of 3.5 μJy at 3.6 μm and 100 μJy at 24 μm.

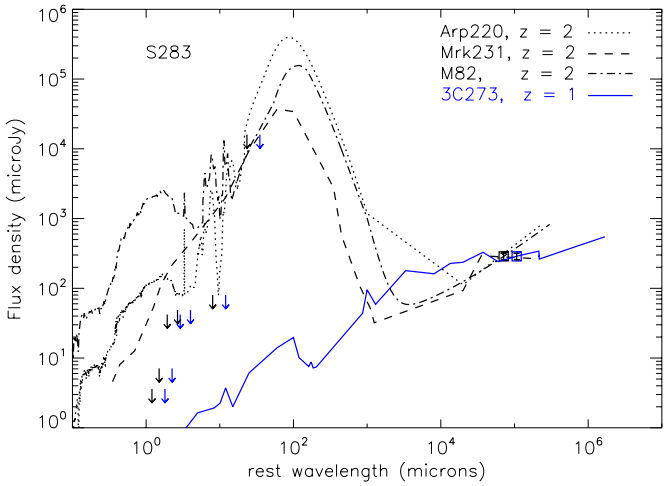

Figure 3. SED of S283, fitted by Arp 220, Mrk 231, M82, and 3C273. Points in black assume the galaxy is at $z = 2$, and blue are the data for $z = 1$. This galaxy is not well fitted by M82, Arp 220, or Mrk 231, as would be detected by IRAC and 24 μm imaging. The SED of radio-loud galaxy 3C273 at $z > 1$ is consistent with the observations. The SEDs are scaled up in luminosity by 90, 12, and 2000 times for Arp 220, Mrk 231, and M82, respectively, and 3C273 is scaled down by a factor of 1800.

If this source was a typical ULIRG like Arp 220 or Mrk 231, even for $z > 2$, it would be detected by IRAC imaging (see Figure 3). For $z < 2$ the 24 μm flux density expected is $\gg 100$ μJy, so it would be clearly detected in MIPS. A star-forming galaxy such as M82 would also have clearly been detected by *Spitzer*. While a redshift less than 1 is allowed by the 3C273 SED that would imply a low-mass object. The stellar mass estimate at $z = 1$ is $M \sim 6 \times 10^9\, M_{\odot}$ assuming the *K*-band luminosity from the 3C273 SED fit and a mass-to-light ratio of 1 (e.g., Bell & de Jong 2001; Lee 2006). This is comparable to the most massive dwarf galaxies, which are

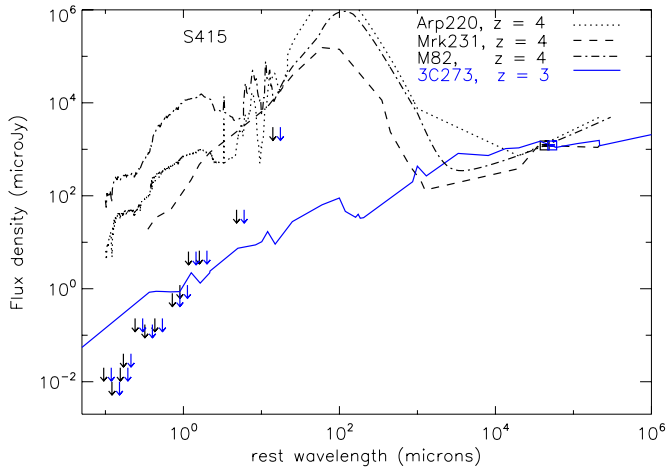

Figure 4. SED of S415, fitted by Arp 220, Mrk 231, M82 and 3C273. Points in black assume the galaxy is at $z = 4$, and blue are the data for $z = 3$. This galaxy is not well fitted by M82, Arp 220, or Mrk 231, as would be detected by *Spitzer* imaging. The SED of radio-loud galaxy 3C273 at $z \gg 1$ is consistent with the observations, if obscuration at optical wavelengths is assumed. The SEDs are scaled up in luminosity by 2.7×10^6, 3.9×10^5, and 6.0×10^7 times for Arp 220, Mrk 231, and M82, respectively, and 3C273 is scaled down by a factor of 30.

(A color version of this figure is available in the online journal.)

not known to be strong radio emitters or contain AGNs. The IRAC limits alone suggest a stellar mass of $M \lesssim 6 \times 10^{10}\,M_\odot$ at $z = 1$. Radio-loud AGNs with SEDs similar to 3C273 are found in massive galaxies with $M > 10^{11}\,M_\odot$. The IRAC non-detection therefore suggests S283 is a radio-loud AGN at $z > 1$. This is supported by the galaxy's MIR–radio correlation, $q = \log(S_{24\,\mu\mathrm{m}}/S_{1.4\,\mathrm{GHz}}) < -0.46$, which is well in the range expected for radio-loud AGNs (e.g., Boyle et al. 2007).

3.2. S415

This IFRS has a flux density of 1.21 mJy at 1.4 GHz, but is undetected in all *Spitzer* bands. Since it lies in the GOODS-S proper, where the data are most sensitive, it has by far the most extreme flux density ratios of the sources discussed here. It is as extreme, if not more so, than the optically faint but submillimeter bright HDF 850.1 (Dunlop et al. 2004; Cowie et al. 2009). This radio source has no ACS counterpart and we measured the 3σ ACS limits at the source position to be $B_{\mathrm{AB}} \gtrsim 28.1$. $V_{\mathrm{AB}} \gtrsim 28.9$, $I_{\mathrm{AB}} \gtrsim 28.3$, and $z_{\mathrm{AB}} \gtrsim 27.4$, using a $0\farcs6$ diameter aperture. There is no NIR counterpart in the MUSYC or VLT ISAAC observations, giving 3σ limits of $J_{\mathrm{AB}} \gtrsim 25.5$, $H_{\mathrm{AB}} \gtrsim 25.8$, and $Ks_{\mathrm{AB}} \gtrsim 25.5$.

If this source has an SED similar to M82, Arp 220, or Mrk 231, it would be detected in all *Spitzer* bands, even 70 μm, for $z < 4$. If the radio-loud 3C273 SED is adopted, this source must lie at $z \gtrsim 3$ for it to remain undetected in the IRAC and ACS bands (assuming no obscuration, see Figure 4). At redshift $z = 1$, the IRAC 3.6 and 4.5 μm limits are a factor of 2–3 below the 3C273 SED, which implies an extinction of 0.8–1.1 mag would be required for this source to be undetected in the IRAC channels. This level of extinction is seen in some extreme ULIRGs (e.g., Genzel et al. 1998; Murphy et al. 2001), but this source is not luminous in the infrared. This source therefore lies at redshift $z \gg 1$. Even at these redshifts obscuration of a few magnitudes is required for a 3C273 object to be undetectable in the optical/NIR bands (see Figure 4). At $z \gtrsim 1$ the radio luminosity of S415 is $P_{1.4\,\mathrm{GHz}} > 5 \times 10^{24}$ W Hz^{-1}. The *Spitzer* non-detection of S415 therefore suggests that this source is a distant ($z \gg 1$) obscured radio-loud AGN.

The X-ray non-detection implies that this source has an X-ray luminosity $L_{0.5-8\,\mathrm{keV}} \lesssim 2 \times 10^{42}$ erg s^{-1} at $z = 2$ and $L_{0.5-8\,\mathrm{keV}} \lesssim 6 \times 10^{42}$ erg s^{-1} at $z = 3$, where the Luo et al. (2008) limit assumes an X-ray power law of $\Gamma = 1.4$. This suggests that, for these redshifts, either the source has a very high column density of neutral hydrogen obscuring the X-ray emission, which is consistent with the optical/NIR non-detection, or the source is intrinsically X-ray faint for an AGN.

A preliminary analysis of ATCA 2.4 GHz data (E. Middelberg et al., in preparation) finds S415 has a significant detection ($>7\sigma$) of 0.67 mJy. This implies a steep radio spectral slope of $\alpha = -1.1$,[6] which cannot be produced by star-forming processes. S415 has a slope similar to some ultra-steep spectrum sources (Rottgering et al. 1997; De Breuck et al. 2004), which have been linked to massive high-redshift ($z > 2$) radio galaxies.

3.3. S446

IFRS S446 is a 0.338 mJy radio source which lies just outside the GEMS ACS coverage and MUSYC NIR imaging. There is a faint source in the IRAC 3.6 and 4.5 μm channels just 2.2 arcsec north of the radio position (see Figure 1) and we assume this is the counterpart to S446. The probability that one or more IRAC sources lies randomly within a distance θ of a radio source is $P = 1 - \exp(-\pi n \theta^2)$, for an IRAC source density n (often called the P-statistic; e.g., Downes et al. 1986). The P-statistic is only a rough estimate because it does not take into account the individual positional uncertainties and assumes a random distribution of the background population, whereas astronomical sources are clustered. Nevertheless, for the SIMPLE IRAC source density of 116,700 deg^{-2} the P-statistic suggests that the chance of an IRAC source lying closer than 2.2 arcsec is 13%, so the counterpart is reasonably reliable. The source is 6.6 ± 0.3 μJy and 5.7 ± 0.5 μJy at 3.6 and 4.5 μm, respectively, and not detected in the other IRAC bands. There is no detection in the 70 and 24 μm images, but limits are hard to quantify because the source falls in between two brighter sources. We assume the noise here is twice that of the local noise in the MIPS imaging for the purposes of the SED fitting.

Similar to the other IFRS sources, the non-detection in the two longer wavelength IRAC bands, and MIPS 24 and 70 μm bands, rules out M82, Arp 220, and Mrk 231 SEDs for this source, at a wide range of redshift ($z < 6$). A 3C273 SED would not produce the MIR emission detected in the IRAC bands (see Figure 5), so a possible explanation for this source is a radio-loud AGN which dominates the radio emission but with a stellar component which is seen in the MIR.

The Maraston (2005) old stellar population fit to the IRAC data constrains the redshift of this galaxy to 1–1.5, and the best fit is a 1 Gyr old model at $z = 1.5$. At this redshift the radio luminosity of S446 is $P_{1.4\,\mathrm{GHz}} = 3.7 \times 10^{24}$ W Hz^{-1}, which would place it at the low-power end of radio-loud AGN.

Using Maraston (2005) SEDs with a different metallicity, including a different library of SEDs (e.g., Bruzual & Charlot 2003), or adding reddening as a free parameter would give a different best-fit redshift, but this level of complexity cannot be explored with only two data points. Finally, we note that the IRAC detections are unlikely to be caused by the hot dust

[6] $S \propto \nu^{\alpha}$.

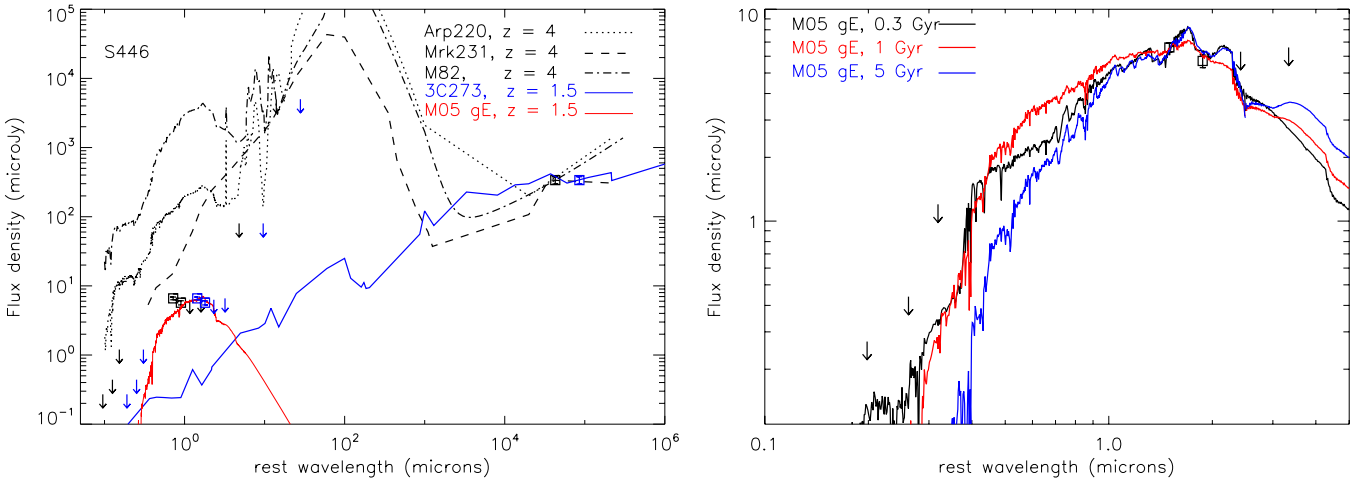

Figure 5. Left: SED of S446, fitted by Arp 220, Mrk 231, M82, and 3C273. The SEDs are scaled up in luminosity by 750, 110, and 17,000 times for Arp 220, Mrk 231, and M82, respectively, and 3C273 is scaled down by a factor of 550. An old stellar population (red line) from Maraston (2005) is fitted to the IRAC data. Points in black assume the galaxy is at $z = 4$, and blue are the data for $z = 1.5$. This galaxy is not well fitted by M82, Arp 220, or Mrk 231, as would be detected by 24 μm imaging. The SED of radio-loud galaxy 3C273 at $z \sim 2.0$ combined with the old stellar population is consistent with the observations. Right: a zoom of the optical/NIR region. The Maraston (2005) stellar population models are shown at the best-fit redshift of 1.5. The 0.3 and 5 Gyr models are satisfactory fits, but the 1 Gyr model provides the best fit. The optical limits are *g*, *r*, and *i* limits from SWIRE.

component of an AGN torus. The IRAC detections imply the MIR peak is shorter than 3.6 μm, so the dust temperatures would be greater than ~1600 K at $z = 1$ and greater than ~2400 K at $z = 2$, using Wien's law. Silicate grains sublimate at about 1000 K, while graphite grains sublimate around 1500 K, so these temperatures are too high for an AGN torus. Instead, AGN torus models typically show a cooler MIR emission peak of 7–10 μm (e.g., Schartmann et al. 2005), which is longward of IRAC channels 1 and 2.

3.4. S506

This source is similar to S446. This 0.170 mJy radio source has a GEMS ACS *V* and *z* band detection 1.″4 south of the radio position that is 26.27 and 25.62 AB magnitudes, respectively (see Figure 1). The likely counterpart in the IRAC 3.6 and 4.5 μm channels is less than 1″ away from the ACS source, roughly 2.″3 south of the radio position. This ACS counterpart, while faint, is a 7.0 and 5.1σ detection in the *V* and *z* bands, respectively.

The *P*-statistic suggests the chance of this IRAC source being a random coincidence is about 14%. The source is 5.5 ± 0.3 μJy and 5.5 ± 0.4 μJy at 3.6 and 4.5 μm, respectively, and not detected in the other IRAC bands. There is no MIPS 70 or 24 μm detection in the FIDEL images of this source. The FIDEL image shows a possible 24 μm excess but this has a flux density of only 7.3 ± 4.2 μJy and is not coincident with the IRAC source. There is also no detection in the MUSYC NIR imaging ($J_{AB} \gtrsim 22.5$ and $K_{AB} \gtrsim 22.0$). Again, M82, Arp 220, and Mrk 231 type SEDs are ruled out for this source by the non-detection in the MIPS 24 and 70 μm bands. The MIR peak is between 3.6 and 4.5 μm and if hot dust is responsible for this then Wien's law implies hot dust temperatures of ~1400 K at redshift 1 and ~2200 K at redshift 2. Similar to S446, this rules out the IRAC detection of a hot AGN tori. The most likely explanation for this source is a radio-loud AGN at ($z > 2$) with a stellar component dominating the IRAC channels (Figure 6).

Using the IRAC data alone, we find the best-fit Maraston (2005) old stellar population model to the IRAC data is 1 Gyr old and places this galaxy at $z = 2.5$. The 5 Gyr model has a redder SED that would be detected by IRAC 5.8 μm imaging at $z < 2$, and the 1 Gyr model becomes a bad fit for $z > 2.6$. However, the ACS detection suggests a blue excess from star formation activity. The best-fit stellar population model to both ACS and IRAC detections is a 0.3 Gyr Maraston (2005) model at $z = 2.0$. As for S446, the small number of data points does not warrant exploring all the free parameters in the redshift fitting, such as metallicity and reddening. However, SEDs younger than 0.3 Gyr were also explored for S506 and these young SEDs have a blue excess inconsistent with the faintness of S506 in the optical bands. At the best-fit redshift of $z = 2.0$, S506 has a radio luminosity $P_{1.4\,GHz} = 3.6 \times 10^{24}$ W Hz^{-1}, which, similar to S446, would place it at the low-power end of radio-loud AGNs.

The ACS counterpart is made up of two clumps (see Figure 1), one of which is extended and has faint emission over 0.3 arcsec, which is 2.5 kpc at redshift $z = 2$. The dual nature of S506 could be explained by one component having an AGN, while one (or both) has some recent star formation.

3.5. IR–Radio Correlation

The IR–radio correlation (e.g., Yun et al. 2001) is an indicator of the dominant emission mechanism in a galaxy because both IR and radio emission are thought to be strongly linked to star formation. Any deviation from the correlation is a sign of an AGN. Galaxies with excess radio emission probably contain a radio-loud AGN, while IR-excess sources are likely to be radio-quiet AGNs with hot dust dominating in the MIR (for $z > 1$). The observed MIPS to radio flux density ratio limits are shown in Figure 7. Some of the xFLS galaxies (Frayer et al. 2006) have ratios consistent with the IFRSs but all are easily detected at optical and infrared wavelengths. The $S_{24\mu m}/S_{1.4\,GHz}$ limits for all four IFRSs show that they have excess radio emission for $z \lesssim 2$. The limits from 70 μm are not as stringent as that from 24 μm, but they do show that the IFRSs have as much excess radio emission as the AGN-dominated ULIRG Mrk 231. The extreme source S415 has a ratio that is consistent with a radio-loud AGN at $z \gtrsim 4$. The IFRS IR–radio ratios are consistent with a sample of high-redshift radio galaxies (HzRGs; Seymour et al. 2007), which host luminous radio-loud AGNs.

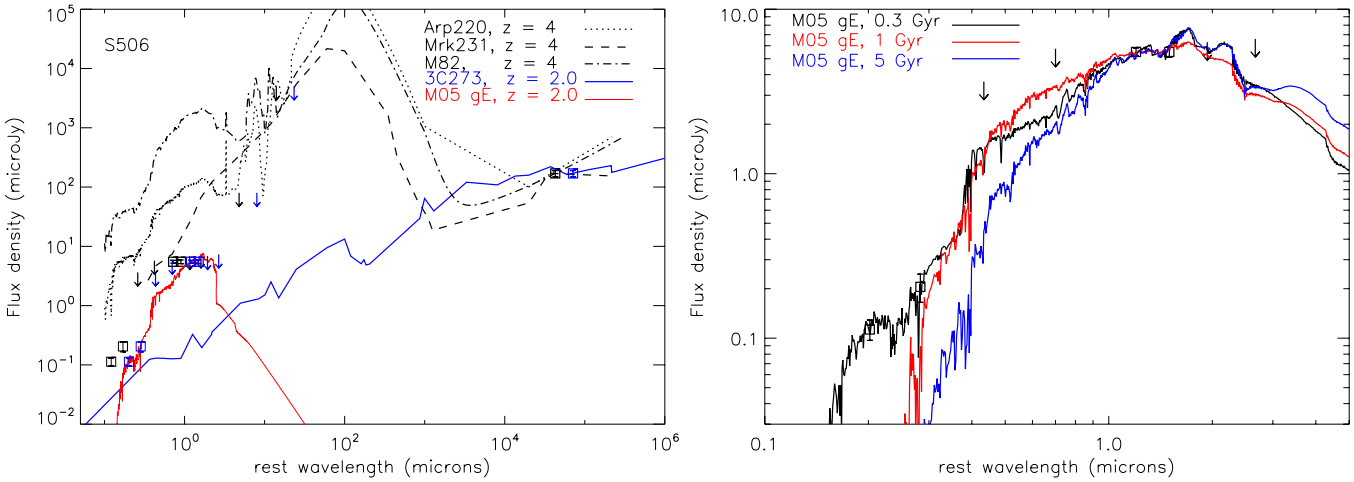

Figure 6. Left: SED of S506, fitted by Arp 220, Mrk 231, M82, and 3C273. The SEDs are scaled up in luminosity by 380, 55, and 8500 times for Arp 220, Mrk 231, and M82, respectively, and 3C273 is scaled down by a factor of 530. An old stellar population (red line) from Maraston (2005) is fitted to the IRAC data. Points in black assume the galaxy is at $z = 4$, and blue are the data for $z = 2.0$. This galaxy is not well fitted by M82, Arp 220, or Mrk 231, as would be detected by 24 μm imaging. The SED of radio-loud galaxy 3C273 at $z \sim 2.0$ combined with the old stellar population is consistent with the observations. Right: a zoom of the optical/NIR region. The Maraston (2005) stellar population models are shown at the best-fit redshift of 2.0. The 1 and 5 Gyr models fit the IRAC data, but only the 0.3 Gyr model (black line) can reproduce both IRAC and ACS detections. The *J* and *K* limits are from MUSYC.

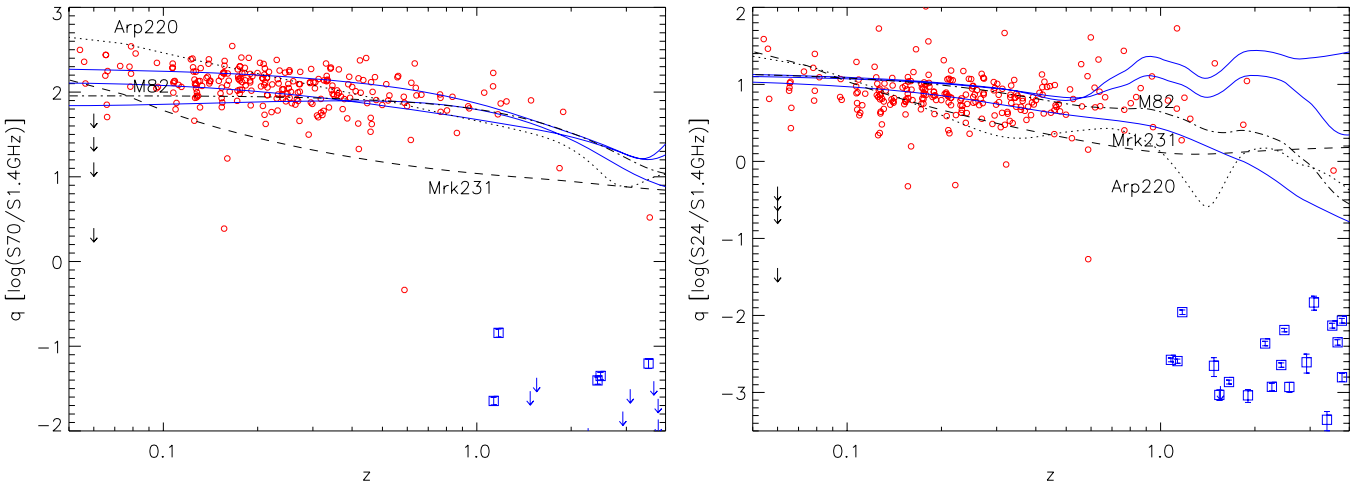

Figure 7. Ratio of *Spitzer* 70 (left) and 24 (right) μm to 1.4 GHz flux density, q, as a function of redshift. The four IFRSs are shown as black arrows at $z = 0.06$, as we have limits only. Red circles are xFLS galaxies (Frayer et al. 2006), which are predominately star-forming galaxies. Blue boxes or arrows show ratios from a sample of HzRGs (Seymour et al. 2007), which are radio-loud AGNs. The black SED tracks are Arp 220 (dotted), Mrk 231 (dashed), and M82 (dot-dashed). Blue solid lines show tracks from Chary & Elbaz (2001) with bolometric IR luminosities ranging from 10^8 to 10^{13} $L_\odot$.

3.6. Could IFRSs be Galactic Objects?

We now consider whether IFRSs may be galactic objects such as pulsars or radio stars. The majority of known pulsars are young objects with a low spin rate and these are distributed across the Galactic disk, as expected for objects that have originated fairly recently from massive stellar supernovae. They are rare objects at high galactic latitude. For example, the Parkes Multibeam Pulsar Survey, with a 1.4 GHz flux density limit of 0.15 mJy for long period pulsars, finds a density of about 1 deg^{-2} for $|b| < 1$ (Camilo et al. 2000). The density of these pulsars drops to <0.25 deg^{-2} by $|b| = 4$ deg. Applying the *P*-statistic from Section 3.3, we find that the probability of one or more pulsars within 15 arcmin (half the eCDFS size) of a radio position is less than 5%, assuming a pulsar density of <0.25 deg^{-2}. The eCDFS has a galactic latitude of about −55 degrees, so the space density of pulsars in the eCDFS field is much less than that. Therefore, the 0.25 degree eCDFS field is unlikely to contain a pulsar.

Shorter period pulsars, so-called millisecond pulsars, are thought to have been spun up to high rotation rates as a member of a low-mass X-ray binary (LMXB) system. These objects are usually found in globular clusters (e.g., Manchester et al. 2001). The eCDFS is not a globular cluster field and so is unlikely to contain an LMXB.

The optical non-detection of the radio sources gives us another clue about whether the sources are pulsars. Neutron stars have been detected in the optical, and we can take two examples: the Crab pulsar and the Vela pulsar. The Crab pulsar's optical counterpart is known as Baade's star and is relatively bright in the optical, with $V = 16.6$. The Crab pulsar lies at 2 kpc (Manchester et al. 2005), so at 10 kpc it would have $V = 20.1$ and $V = 25.1$ at 100 kpc. Thus, if these IFRSs are as bright as the Crab pulsar in the optical, they would be easily detectable

in the optical imaging. The Vela pulsar is much fainter however, $V = 23.6$ (Mignani & Caraveo 2001), and lies at a distance of 294 pc (Caraveo et al. 2001). An object such as this would be too faint for eCDFS *Hubble Space Telescope* detection if it lies further than about 2.3 kpc.

X-ray emission from the neutron star surface or from the pulsar wind nebula may be detectable if the IFRS is a pulsar. The one source with X-ray data, S415, has an X-ray luminosity limit that is 100 times less than some of the faintest X-ray emitting pulsars known (e.g., Kargaltsev & Pavlov 2009). X-ray emission from a neutron star may not be orientated the same way as the radio emission, and the X-ray–radio observations were not simultaneous, so this is not conclusive evidence that S415 is not a pulsar. It is however consistent with the idea that S415 is an extragalactic source.

Could IFRSs be main-sequence stars? Ultracool dwarf stars, a class thought to be radioactive, were observed at 4.8 GHz, but only one was detected in a survey of eight (Antonova et al. 2008). This star lies at a distance of 12.2 pc and has a 4.8 GHz flux density of 0.286 mJy. Berger (2006) observed 90 M and brown dwarf stars and found 8.5 GHz flux densities well below 1 mJy, although flares can increase the flux density by at least a factor of a few. The stars in this sample are all closer than about 13 pc and have J and K magnitudes brighter than 18 mag. The typical M-dwarf has an absolute magnitude of 8–17 M_V (e.g., Kaler 1997), so at a distance of 1 kpc (10 kpc) M-dwarfs have an observed magnitude of $V = 18$–27 (23.1–32.1). Therefore, the weakest of these would be undetected in the optical images at large distances, but the radio studies suggest M-dwarf stars close enough to be detected in the radio would be seen in the optical images.

3.7. Comparison to Other Galaxy Populations

We can compare the space density of our sample of IFRSs with that of other high-redshift $z \sim 2$ samples. For example, much work has been done on the BzK selection technique (Daddi et al. 2004) to select star-forming and passive galaxies at $z \sim 2$. The space density of BzKs is $\sim$1 per arcmin^2 (Daddi et al. 2007), more than 200 times greater than that of the IFRSs in this work ($\sim$16 deg^{-2}).

Another high-redshift sample is dust-obscured galaxies (DOGs), which are selected using a combination of red colors ($R - [24] > 14$, in Vega magnitudes) and bright flux densities in infrared ($S_{24} > 0.3$ mJy) (Dey et al. 2008). These criteria proved remarkably efficient for selecting $z \sim 2$ galaxies. DOGs contribute $\sim$26% of the total IR luminosity density at $z = 2$ and 60% of the total from ULIRGs. They have a space density of $\sim$0.1 per arcmin^2 or $2.82 \pm 0.05 \times 10^{-5}$ h^3 Mpc^{-3}, similar to submillimeter galaxies and about 20 times more numerous than the IFRSs.

The paucity of IFRSs is not a surprise as they were selected to have extreme radio to infrared ratios, and as such are rare compared to other populations selected in the optical and infrared. How do AGN samples selected in the radio compare? By matching Faint Images of the Radio Sky at Twenty-cm (FIRST) 1.4 GHz radio sources with the Sloan Digital Sky Survey (SDSS), Ivezić et al. (2002) find about three radio-selected AGN deg^{-2} with $S_{1.4} > 1$ mJy and $i < 21$. The four IFRSs in this study, likely radio-loud AGNs at $z > 1$, have a source density $\sim$16 deg^{-2}. This suggests that IFRSs are a population of radio-loud AGNs which have been unstudied by previous radio work.

S446 and S506 lie at redshifts 1 to 2 and have radio powers ($P_{1.4\,\mathrm{GHz}}$) of $\sim 10^{24}$ W Hz^{-1}. The local luminosity function of radio AGN (Best et al. 2005; Sadler et al. 2002) suggests that there are 40–60 AGNs deg^{-2} with radio powers of 10^{24}–10^{25} W Hz^{-1} in the volume between redshifts 1 to 2, assuming no evolution. If luminosity evolution (e.g., Donoso et al. 2009; Sadler et al. 2007) is applied, the number of AGNs with radio powers of 10^{24}–10^{25} W Hz^{-1} increases to 110–140 deg^{-2}. Therefore, the IFRSs presented in this work make up only a small portion ($\lesssim 1\%$) of the total AGN population with similar radio powers at that epoch. The remainder are presumably bright enough to be detected in the *Spitzer* bands.

The IFRSs can also be compared to HzRGs. A representative sample of 69 HzRGs at $z > 1$ were observed with *Spitzer* (Seymour et al. 2007) and these massive galaxies (10^{11}–$10^{11.5}$ $M_\odot$) have the MIR luminosities of LIRGs or ULIRGs. While HzRGs have much greater radio flux densities than IFRSs, they have extreme MIR–radio ratios consistent with the available data on IFRSs (Figure 7). Hence, IFRSs may be the lower luminosity analogs of HzRGs. There are only a few hundred known HzRGs across the full sky, so they are even rarer than IFRSs.

4. SUMMARY

We have searched for infrared counterparts to four IFRSs in the eCDFS field using recently available ultra-deep *Spitzer* observations. No IFRS is detected in ultra-deep 24 μm imaging, implying that the sources do not follow the IR–radio correlation and star formation cannot produce all the radio emission observed in these objects. We find IRAC detections for two of the sources, and the non-detections of the other two provide constraints on the source SEDs. Typical ULIRG SEDs, such as Mrk 231 and Arp 220, and L_* galaxies are ruled out by the *Spitzer* data. The most likely explanation for these sources is that they are radio-loud AGNs, with radio-to-optical ratios similar to 3C273, at redshifts $z \gtrsim 1$. The most extreme source (S415) lies at $z \gg 1$ and requires several magnitudes of obscuration in the optical/NIR to remain undetected by deep imaging. It is very unlikely that the IFRSs are Galactic sources, but current data cannot conclusively rule this out in the case of the undetected sources.

For the two sources with IRAC detections we find the SED can be described by a radio-loud 3C273-like SED combined with a stellar population. The stellar population SED fits to the IRAC MIR data, combined with the available optical limits, suggest that the two detected IFRS sources have redshifts of $z \sim 1.5$ and $z \sim 2.0$. For one source, S506, the ACS detection suggests the galaxy may have a stellar component that is only 0.3 Gyr in age. These two sources are similar to the IRAC-detected OIRSs which are posited to be "red and dead" radio galaxies at $z > 1$ (Higdon et al. 2008).

The evidence is mounting that a significant proportion, if not all, of the IFRS sources are radio-loud AGNs at high redshift ($z \gtrsim 1$), and not merely lobes of an unidentified radio galaxy. The source density in eCDFS is $\sim$16 deg^{-2} for $S_{1.4} > 0.1$ mJy. Garn & Alexander (2008) find a source density of $\sim$3.5 deg^{-2} for $S_{1.4} > 0.5$ mJy. While these sources are rare, they point to a population of AGNs at high redshift that has been undiscovered until recently.

This work is based in part on observations made with the *Spitzer Space Telescope*, which is operated by the Jet Propulsion Laboratory, California Institute of Technology under

a contract with NASA. Support for this work was provided by NASA through an award issued by JPL/Caltech. This research has made use of the NASA/IPAC Extragalactic Database (NED) which is operated by the Jet Propulsion Laboratory, California Institute of Technology, under contract with the National Aeronautics and Space Administration.

REFERENCES

Antonova, A., Doyle, J. G., Hallinan, G., Bourke, S., & Golden, A. 2008, A&A, 487, 317
Bell, E. F., & de Jong, R. S. 2001, ApJ, 550, 212
Berger, E. 2006, ApJ, 648, 629
Best, P. N., Kauffmann, G., Heckman, T. M., & Ivezić, Ž. 2005, MNRAS, 362, 9
Boyle, B. J., Cornwell, T. J., Middelberg, E., Norris, R. P., Appleton, P. N., & Smail, I. 2007, MNRAS, 376, 1182
Bruzual, G., & Charlot, S. 2003, MNRAS, 344, 1000
Camilo, F., et al. 2000, in ASP Conf. Ser. 202, Pulsar Astronomy—2000 and Beyond, ed. M. Kramer, N. Wex, & R. Wielebinski (San Francisco, CA: ASP), 3
Caraveo, P. A., De Luca, A., Mignani, R. P., & Bignami, G. F. 2001, ApJ, 561, 930
Chary, R., & Elbaz, D. 2001, ApJ, 556, 562
Cowie, L. L., Barger, A. J., Wang, W.-H., & Williams, J. P. 2009, ApJ, 697, L122
Daddi, E., Cimatti, A., Renzini, A., Fontana, A., Mignoli, M., Pozzetti, L., Tozzi, P., & Zamorani, G. 2004, ApJ, 617, 746
Daddi, E., et al. 2007, ApJ, 670, 156
De Breuck, C., Hunstead, R. W., Sadler, E. M., Rocca-Volmerange, B., & Klamer, I. 2004, MNRAS, 347, 837
Dey, A., et al. 2008, ApJ, 677, 943
Donoso, E., Best, P. N., & Kauffmann, G. 2009, MNRAS, 392, 617
Downes, A. J. B., Peacock, J. A., Savage, A., & Carrie, D. R. 1986, MNRAS, 218, 31
Dunlop, J. S., et al. 2004, MNRAS, 350, 769
Frayer, D. T., et al. 2006, AJ, 131, 250
Garn, T., & Alexander, P. 2008, MNRAS, 391, 1000
Gawiser, E., et al. 2006, ApJS, 162, 1
Genzel, R., et al. 1998, ApJ, 498, 579
Giacconi, R., et al. 2002, ApJS, 139, 369
Giavalisco, M., et al. 2004, ApJ, 600, L93
Higdon, J. L., Higdon, S. J. U., Willner, S. P., Brown, M. J. I., Stern, D., Le Floc'h, E., & Eisenhardt, P. 2008, ApJ, 688, 885
Higdon, J. L., et al. 2005, ApJ, 626, 58
Ivezić, Ž., et al. 2002, AJ, 124, 2364
Kaler, J. B. 1997, Stars and their Spectra: An Introduction to the Spectral Sequence (Cambridge: Cambridge Univ. Press)
Kargaltsev, O., & Pavlov, G. G. 2009, ApJ, 702, 433
Lee, H., et al. 2006, ApJ, 647, 970
Lonsdale, C., et al. 2004, ApJS, 154, 54
Luo, B., et al. 2008, ApJS, 179, 19
Manchester, R. N., Hobbs, G. B., Teoh, A., & Hobbs, M. 2005, AJ, 129, 1993
Manchester, R. N., et al. 2001, MNRAS, 328, 17
Maraston, C. 2005, MNRAS, 362, 799
Middelberg, E., Norris, R. P., Tingay, S., Mao, M. Y., Phillips, C. J., & Hotan, A. W. 2008a, A&A, 491, 435
Middelberg, E., et al. 2008b, AJ, 135, 1276
Mignani, R. P., & Caraveo, P. A. 2001, A&A, 376, 213
Murphy, T. W., Jr., Soifer, B. T., Matthews, K., Armus, L., & Kiger, J. R. 2001, AJ, 121, 97
Norris, R. P., Tingay, S., Phillips, C., Middelberg, E., Deller, A., & Appleton, P. N. 2007, MNRAS, 378, 1434
Norris, R. P., et al. 2006, AJ, 132, 2409
Rix, H.-W., et al. 2004, ApJS, 152, 163
Rottgering, H. J. A., van Ojik, R., Miley, G. K., Chambers, K. C., van Breugel, W. J. M., & de Koff, S. 1997, A&A, 326, 505
Sadler, E. M., et al. 2002, MNRAS, 329, 227
Sadler, E. M., et al. 2007, MNRAS, 381, 211
Schartmann, M., Meisenheimer, K., Camenzind, M., Wolf, S., & Henning, T. 2005, A&A, 437, 861
Seymour, N., et al. 2007, ApJS, 171, 353
Silva, L., Granato, G. L., Bressan, A., & Danese, L. 1998, ApJ, 509, 103
Taylor, E. N., et al. 2009, ApJS, 183, 295
Yun, M. S., Reddy, N. A., & Condon, J. J. 2001, ApJ, 554, 803